POF1B Localizes to Desmosomes and Regulates Cell Adhesion in Human Intestinal and Keratinocyte Cell Lines

Arianna Crespi[1], Alessandra Bertoni[1], Ilaria Ferrari[1], Valeria Padovano[1], Pamela Della Mina[2], Emilio Berti[2,3], Antonello Villa[2] and Grazia Pietrini[1]

By means of morphological and biochemical criteria, we here provide evidence for the localization and function of premature ovarian failure, 1B (POF1B) in desmosomes. In monolayers of Caco-2 intestinal cells and in stratified HaCaT keratinocytes, endogenous POF1B colocalized with desmoplakin at desmosome plaques and in cytoplasmic particles aligned along intermediate filaments (IFs). POF1B predominantly co-fractionated with desmosomes and IF components and exhibited properties characteristic of desmosomes (i.e., detergent insolubility and calcium independence). The role of NH_2 and COOH domains in the association of POF1B with desmosomes and IFs was revealed by transient expression of the truncated protein in Caco-2 cells and in cells lacking desmosomes. The function of POF1B in desmosomes was investigated in HaCaT keratinocytes stably downregulated for POF1B expression. Transmission electron microscopy analysis revealed a decrease in desmosome number and size, and desmosomes of the downregulated keratinocytes displayed weak electron-dense plaques. Desmosome alterations were associated with defects in cell adhesion, as revealed by the reduced resistance to mechanical stress in the dispase fragmentation assay. Moreover, desmosome localization of POF1B was restricted to granular layers in human healthy epidermis, whereas it largely increased in hyperproliferative human skin diseases, thus demonstrating the localization of POF1B also in desmosomes of multistratified epithelia.

Journal of Investigative Dermatology (2015) **135,** 192–201; doi:10.1038/jid.2014.327; published online 18 September 2014

INTRODUCTION

Epithelia are formed by sheets of cells organized in a monolayer, as in developing embryos and the gastrointestinal tract, or in stratified multilayers, as in the skin. Epithelial cohesion requires the formation of adhesive contacts named tight junctions (TJs), adherens junctions (AJs), and desmosomes (Capaldo *et al.*, 2014).

Among cell–cell adhesion structures, desmosomes are the most essential for mechanical coupling. Their high degree of adhesive strength is based on multiple, strong, and non-covalent interactions between their molecular constituents. Desmosomes are particularly abundant in skin and cardiac muscle, both of which have to withstand considerable mechanical stress (Kowalczyk and Green, 2013). The mechanical stability of desmosomes depends in large part on their tight association with the intermediate filament (IF) cytoskeleton. Desmosomes are formed by the products of three gene superfamilies: the desmosomal cadherins, the armadillo family, and the plakins. The desmosomal cadherins desmocollins and desmogleins (DSGs) are transmembrane proteins that interact in the extracellular space to couple the two halves of the desmosome. They are linked to IFs through desmoplakin (DSP), plakoglobin (PG), plakophilins (PKPs), and other desmosome-associated proteins (Yin and Green, 2004 and references herein). Together, these proteins form the desmosomal plaque in the intracellular side of the junction. The assembly of proteins anchoring IFs to desmosomal cadherins ensures tissue organization and rigidity (Oriolo *et al.*, 2007).

The importance of desmosomes in the maintenance of strength and flexibility of epithelial tissues is highlighted by mutations in desmosomal genes compromising skin or heart tissues (Bolling and Jonkman, 2009; Brooke *et al.*, 2012). In some instances both of these tissues are affected, as in Naxos disease, a recessively inherited condition with arrhythmogenic right ventricular cardiomyopathy and a cutaneous phenotype (Protonotarios *et al.*, 1986). Interestingly, arrhythmogenic right

[1]*Department of Medical Biotechnology and Translational Medicine, Università degli Studi di Milano and CNR Institute of Neuroscience, Milan, Italy;* [2]*Consorzio MIA and DISS, Università Milano-Bicocca, Milan, Italy and* [3]*Department of Dermatology, Fondazione Ca`Granda, Ospedale Maggiore Policlinico, Milan, Italy*

Correspondence: Grazia Pietrini, Department of Medical Biotechnology and Translational Medicine, Università degli Studi di Milano and CNR Institute of Neuroscience, Via Vanvitelli 32, 20129 Milan, Italy.
E-mail: grazia.pietrini@unimi.it

Abbreviations: AJ, adherens junction; BCC, basal cell carcinoma; C-TER, C-terminal; DSG, desmoglein; DSP, desmoplakin; GFP, green fluorescent protein; IF, intermediate filament; K8–14, keratin 8–14; MDCK, Madin–Darby canine kidney; N-TER, N-terminal; PG, plakoglobin; PKP, plakophilin; POF1B, premature ovarian failure, 1B; PsO, psoriasis; SCC, squamous cell carcinoma; TJ, tight junction

Received 11 December 2013; revised 16 July 2014; accepted 22 July 2014; accepted article preview online 1 August 2014; published online 18 September 2014

ventricular cardiomyopathy is caused mainly by mutations in genes encoding desmosomal proteins (Rampazzo, 2006), but causative genes have not been identified in 40–50% of cases, suggesting that proteins with a role in desmosomes remain to be identified.

The gene encoding premature ovarian failure, 1B (POF1B) maps to the region of the X chromosome critical for normal ovarian function, despite lacking genetic evidence of its role in POF disease (Riva *et al.*, 1996; Bione *et al.*, 2004). POF1B expression is restricted to epithelia, with the highest levels in desmosome-rich tissues such as the epidermis and oropharyngeal and gastrointestinal tracts (Rizzolio *et al.*, 2007). Colocalization of POF1B with desmosomal proteins has been described in human duodenum, but its undetectable expression in the desmosome-enriched spinous layer of epidermis and its enrichment in the granular layer had suggested a role for the protein in TJs and skin terminal differentiation rather than in desmosomes (Rizzolio *et al.*, 2007).

POF1B is a cytosolic protein with a large coiled-coil region in its C-terminal (C-TER) half. The protein is rapidly recruited along the nascent basolateral cell–cell contacts when stably overexpressed in Madin–Darby canine kidney (MDCK) cells (Padovano *et al.*, 2011). In fully polarized MDCK cells, the overexpressed protein localized along the entire lateral junctional domain, with peculiar enrichments in two rings, one apical at the TJ level and one more basal. In line with a role of POF1B in TJs, alterations in the acquisition of transepithelial electrical resistance and monolayer polarization have been documented in MDCK cells overexpressing a human POF–associated mutant characterized by a decreased binding affinity for nonmuscle actin filaments (Lacombe *et al.*, 2006; Padovano *et al.*, 2011). Localization of endogenous POF1B to the entire lateral junctional domain has also been described in human intestinal Caco-2 cells, and downregulation of the protein caused a dramatic loss of the polarized phenotype, suggesting defects in cells' adhesive properties (Padovano *et al.*, 2011).

In order to clarify the specific role of POF1B in cell adhesion, we further characterized the localization and function of the endogenous protein in human cell models of simple (intestinal Caco-2 cells) and stratified (keratinocyte HaCaT cells) epithelia, as well as in normal and in hyperproliferative skin disorders.

RESULTS AND DISCUSSION

Colocalization of POF1B with desmosomal markers in Caco-2 cells

Apical enrichment of POF1B at the level of TJs has been documented in human intestinal Caco-2 cells and in MDCK cells stably expressing the green fluorescent protein (GFP)-tagged protein (Padovano *et al.*, 2011). However, POF1B shows punctate enrichments along the entire cell–cell adhesion surface that nicely colocalize with desmosomal markers both in intestinal sections (Figure 1a and Rizzolio *et al.*, 2007) and in Caco-2 cells (Figure 1b). The apical enrichment of POF1B may represent localization of the protein at TJs or at desmosomes located very close to them, and thus indistinguishable by immunofluorescence. However, POF1B staining in Caco-2 cells is different from the typical indented pattern of the TJ marker claudin 2 or the uniform label of the AJ marker β-catenin (Figure 1b). Colocalization of POF1B with desmosomal proteins was confirmed by analysis of the percentage of staining-free pixels at the plasma membrane (Figure 1c). This quantification reflects the localization pattern of the adhesion markers and shows that the distribution of POF1B is identical only to proteins exclusively found in desmosomes, whereas its distribution is completely different from that of β-catenin and claudin 2, and it only partially resembles that of PG, a protein also found in AJs. The recruitment of POF1B to desmosomes was further suggested by its localization to adhesion sites connected to IFs (Figure 1d).

Detergent insolubility and calcium independence of POF1B and desmosomes in Caco-2 cells

Among cell–cell junctions, desmosomes are characterized by the capability to form insoluble complexes with IFs and to reach a calcium-independent mature state called hyper-adhesion (Garrod and Kimura, 2008). To assess the solubility of POF1B, we performed a Triton X-100 extraction in Caco-2 cells grown confluent for 6 days in regular medium or switched to calcium-deprived medium for the last 30 minutes (Figure 2a). Three consecutive extractions were used to obtain soluble and cytosolic components, actin and tubulin cytoskeleton, chromatin-associated proteins, and the insoluble nuclear matrix–IF fraction (Fey *et al.*, 1984). The majority of POF1B (>60%) co-fractionated with desmosomal components (DSP, DSG) and keratin 8 (K8) and not with markers of AJs (E-cadherin and LIN7) and TJs (occludin, LIN7, PAR3, and claudin 2). Similar to the behavior of desmosome components, the POF1B distribution in the insoluble nuclear matrix–IF fraction was mostly independent on calcium.

Mature hyper-adhesive desmosomes are highly resistant to disruption, whereas TJs and AJs break down upon calcium deprivation (Wallis *et al.*, 2000). Caco-2 cells cultured confluent for >6 days in conventional calcium culture conditions largely lost their contacts when switched to a calcium-free medium for 60 minutes (Figure 2b). Nonetheless, POF1B and DSP or PG and PKP2 (not shown) co-accumulated in the remaining adhesion contacts (arrows) that were devoid of claudin 2 or E-cadherin (not shown).

Collectively, the IF and Triton X-100 insolubility studies clearly indicate a localization of POF1B in desmosomes, although its partial distribution in AJs and TJs cannot be excluded.

Colocalization of POF1B in intracellular particles closely associated with IFs in Caco-2 cells

It is known that DSP and PKP2 form particles that slowly traffic to desmosomes in close association with IFs (Kowalczyk and Green, 2013), whereas intracellular trafficking of PG and DSG is vesicle mediated and microtubule dependent (Green *et al.*, 2010; Nekrasova *et al.*, 2011). We observed staining of POF1B in intracellular particles (red) precisely aligned along

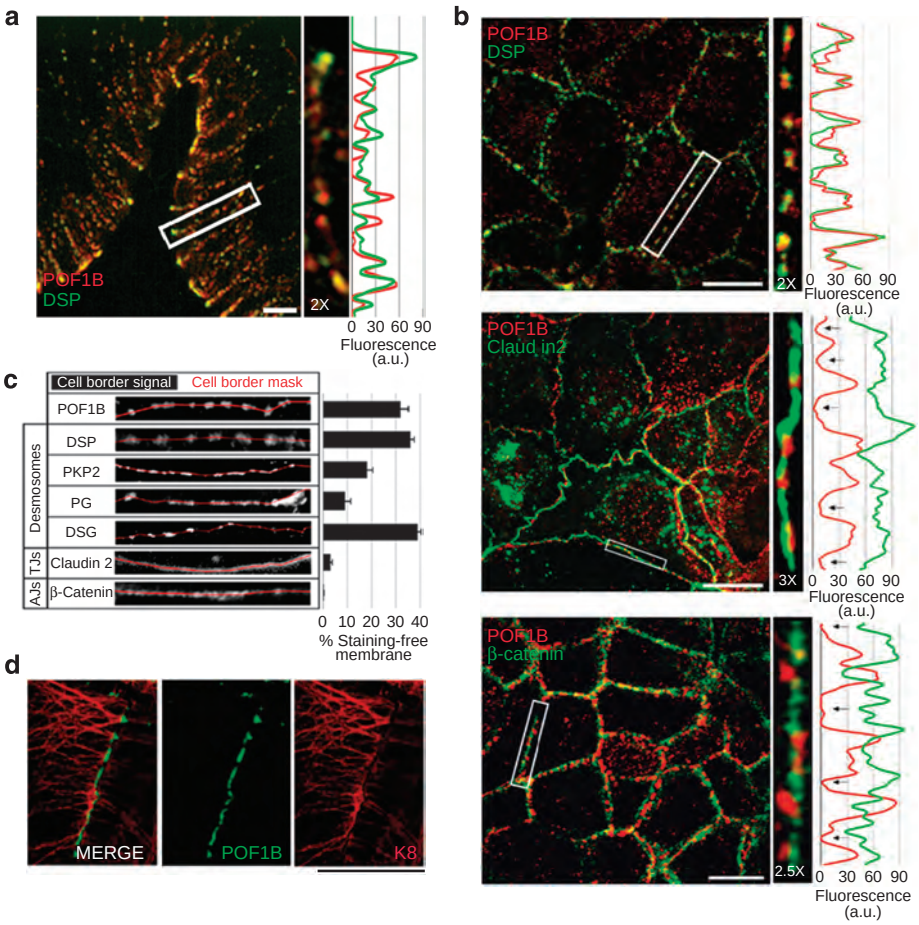

Figure 1. Premature ovarian failure, 1B (POF1B) colocalization with desmosomal proteins in human intestinal Caco-2 cells. (**a**, **b**) Immunofluorescence confocal analysis of human duodenum (**a**) and Caco-2 cells (**b**) probed for endogenous POF1B (red) and the indicated markers of desmosomes, tight junctions (TJs), and adherens junctions (AJs) (green). Fluorescence intensity (in arbitrary units) was analyzed using ''plot profiles.'' Bars = 10 µm. (**c**) Representative images (left) of individual signals in cell–cell adhesion membrane (indicated by the red line) and graph (right) representing the percentage of staining-free membrane (measured in ~100 µm adhesion membranes). (**d**) Individual and merged images of Caco-2 cells co-stained for POF1B (green) and keratin 8 (K8) (red); bar = 5 µm.

keratin filaments (green) in subconfluent Caco-2 cells (Figure 3a), which colocalized with DSP and PKP2 but not with DSG or PG particles (Figure 3b and c). Moreover, when representative strings of particles from each confocal section were magnified and the intensity was analyzed by ''plot profiles'', a clear colocalization of POF1B particles with DSP and PKP2 was revealed, whereas only a portion of particles showed an apparent colocalization with PG. Almost no colocalization was observed between particles of POF1B and DSG, and these results were confirmed by ''surface plot analysis'' (Figure 3c), thus suggesting that POF1B may traffic to the cell–cell contacts in multi-protein complexes in close association with IFs.

Role of the N- and C-terminal domains in the localization of POF1B

We next investigated the role of POF1B domains in its localization. cDNAs encoding for human POF1B full-length, N-terminal (N-TER), and C-TER domains, fused to GFP (Figure 4a), were transiently transfected in Caco-2 cells and in IOSE523 cells, an epithelial cell line of ovarian origin expressing neither DSP (Auersperg *et al.*, 1994) nor PKP2 and PG (data not shown).

In Caco-2 cells, the overexpressed full-length protein localized at cell–cell contact sites connected with IFs (Figure 4b) like the endogenous protein, thus indicating that the GFP tag did not impair the adhesion recruitment of the protein. In the desmosome-deficient IOSE523 cell line, POF1B did not show the cytosolic localization expected for a soluble protein, but a filamentous staining regularly aligned along K8-positive filaments (Figure 4b), indicating that the interaction between POF1B and IFs does not require DSP or PKP2. POF1B N-TER was largely cytosolic with a higher solubility compared with full length, as observed through biochemical fractionation (data not shown). However, POF1B N-TER was also detected at cell–cell contacts in Caco-2 cells (white arrows, Figure 4c) but never in IOSE523 cells. Conversely, the C-TER construct is not recruited to cell–cell contacts but does colocalize with K8 filaments in both Caco-2 and IOSE523 cells (Figure 4d). The N-TER domain of POF1B is therefore necessary and sufficient for interaction with desmosomal components at cell–cell contacts, whereas the C-TER

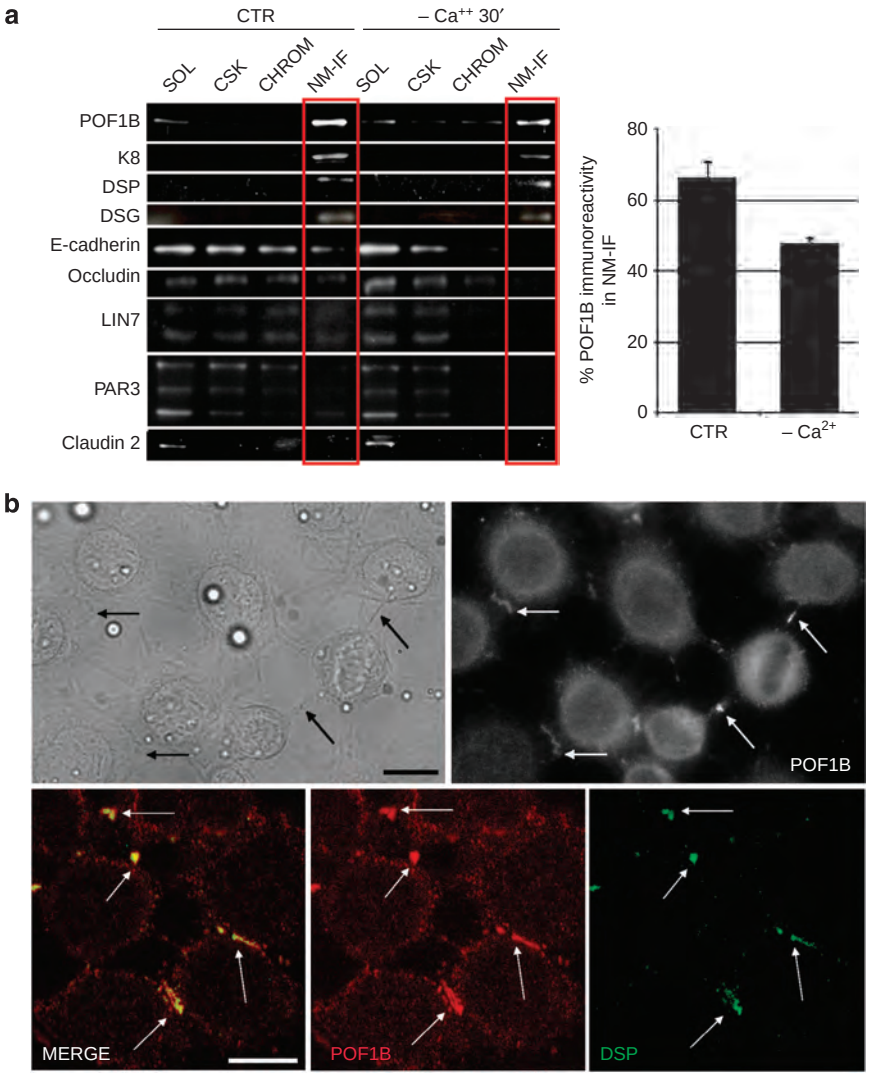

Figure 2. Insolubility and calcium independence of premature ovarian failure, 1B (POF1B) in Caco-2 cells. (**a**) Western blot analysis of subfractions cultured in regular medium (CTR) or in low-calcium medium ($-Ca^{2+}$) for 30 minutes (Fey *et al.*, 1984). Equivalent aliquots from the soluble (SOL), cytoskeleton (CSK), chromatin (CHROM), and nuclear matrix–IF (NM-IF) fractions were loaded onto a 10% SDS-PAGE gel, and the transferred proteins were immunoprobed as indicated (left); (right) quantification of the percentage of POF1B in the NM-IF fraction ± SEM ($n = 3$). (**b**) Top: phase contrast (left) and corresponding single-channel confocal image (right); bottom: a representative calcium-switch experiment performed in Caco-2 cells cultured for 18 days and switched to Ca^{2+}-free medium for 1 hour. Arrows indicate the hyper-adhesive desmosomes. Bars = 10 μm.

domain may mediate the connection with IFs. In addition, the POF1B antibody co-immunoprecipitated endogenous K8 in subconfluent and confluent Caco-2 cells (Figure 4e), further highlighting the association of POF1B with IFs and suggesting that their interaction occurs before adhesion recruitment and is maintained thereafter.

To demonstrate that the observed POF1B filaments are due to association with IFs not requiring DSP or PKP2, K8-specific siRNA was co-transfected with GFP–POF1B into IOSE523 cells (Figure 4f). The K8-targeted siRNA was effective in downregulating the protein (see western blot). GFP–POF1B and K8 lost their typical filamentous distribution, and POF1B showed a cytoplasmic spot-like pattern often colocalizing with residual K8, further suggesting their direct association. As POF1B and DSP are coiled-coil domain-containing proteins able to interact and form filaments with IFs through their C-TER domains, and both are targeted to desmosomes via their amino-terminal domain (Stappenbeck and Green, 1992; Kouklis *et al.*, 1994), these data reveal structural and functional analogies between DSP and POF1B. However, a more labile association of POF1B compared with DSP to IFs is suggested by the higher Triton X-100 solubility and cytosolic localization of POF1B observed under conditions of calcium deprivation (Figure 2a and b).

Generation of stable HaCaT keratinocyte lines silenced for POF1B

Given the crucial role of desmosomes in determining a strong adhesion between adjacent cells, these junctions are especially relevant in tissues that are most subjected to mechanical

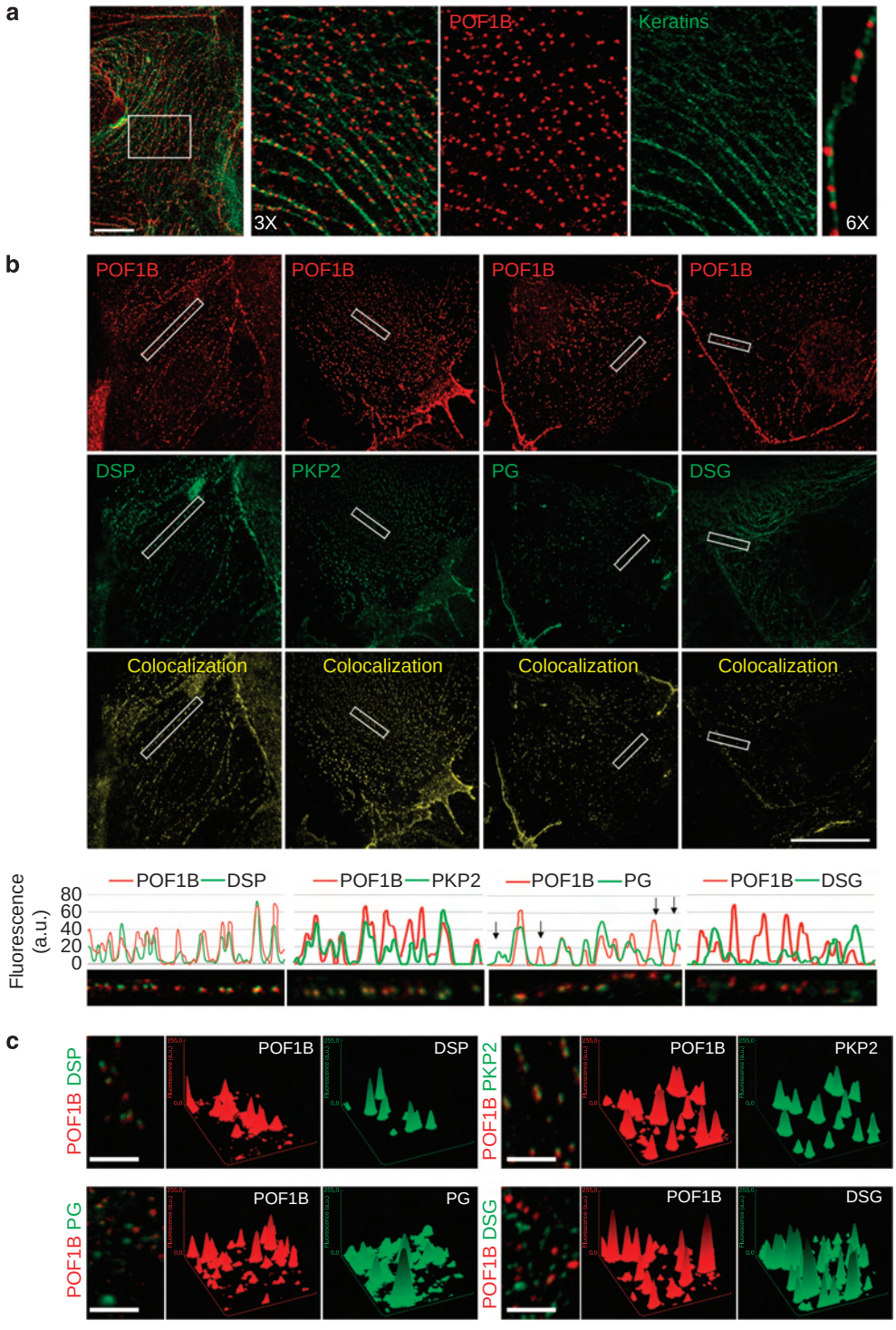

Figure 3. Premature ovarian failure, 1B (POF1B) colocalization with desmosome-associated proteins in cytoplasmic particles aligned along intermediate filaments. (**a**–**c**) Merged and single-channel confocal images in subconfluent Caco-2 cells immunostained for POF1B (red) and the indicated markers (green). (**a**) Low-magnification-merged image and ×3 magnification of merged and single-channel images of POF1B and keratins; a ×6 magnification of one isolated filament is shown on the right; bar = 5 μm. (**b**) Images representing only colocalization signals (yellow); bar = 10 μm. Plot profiles represent signal intensity across boxed insets. (**c**) Surface plot analysis of the merged images. Individual fluorescence peaks are presented; bars = 2 μm.

stress, such as the skin. Accordingly, the desmosome localization of POF1B was investigated in the spontaneously immortalized human keratinocyte line HaCaT. Double immunofluorescence experiments confirmed that POF1B is a *bona fide* desmosome-associated protein, as we measured colocalization of POF1B with DSP (63% ± 3,7) at cell–cell

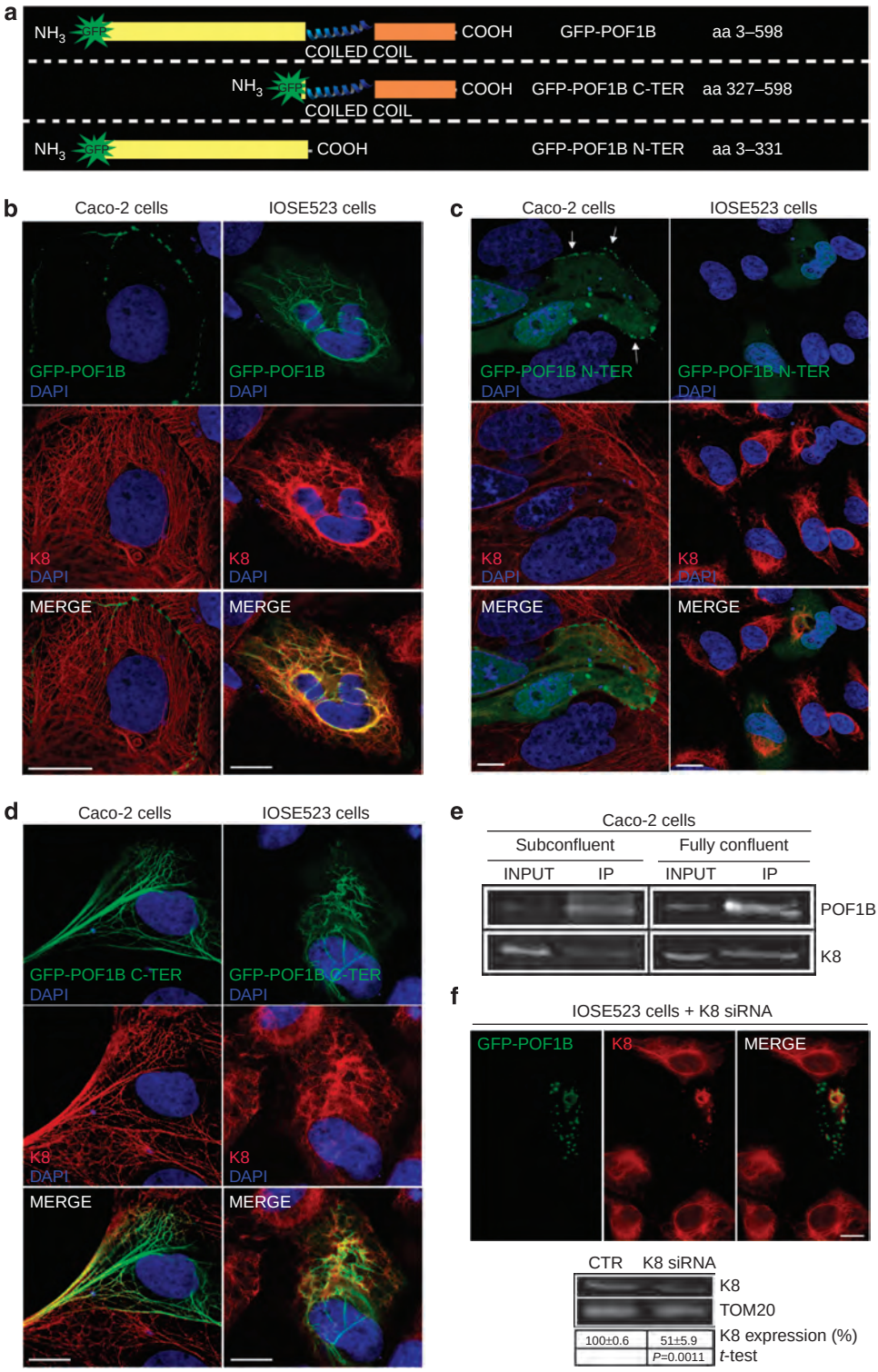

Figure 4. Premature ovarian failure, 1B (POF1B) domains for association with desmosomes and intermediate filaments. (**a**) Representation of green fluorescent protein GFP–POF1B constructs. (**b–d**) Caco-2 and IOSE523 cells transiently transfected with GFP–POF1B (**b**), GFP–POF1B N terminal (N-TER) (**c**), and GFP–POF1B C terminal (C-TER) (**d**) were stained for endogenous keratin 8 (K8) (red) and 4′,6-diamidino-2-phenylindole (DAPI) (blue). Arrows in **c** indicate adhesion sites. (**e**) POF1B immunoprecipitation in subconfluent and confluent Caco-2 cells. Input (2%) and POF1B immunoprecipitates (IP) were analyzed for POF1B and K8. (**f**) IOSE523 cells transiently co-transfected with K8 siRNA and GFP–POF1B cDNAs were stained for K8. The western blot was immunoprobed for K8 and TOM20 as a control. Table represents the K8 expression level in silenced cells normalized to control; data are presented as mean ± SEM ($n = 3$ independent experiments). Bars = 10 μm.

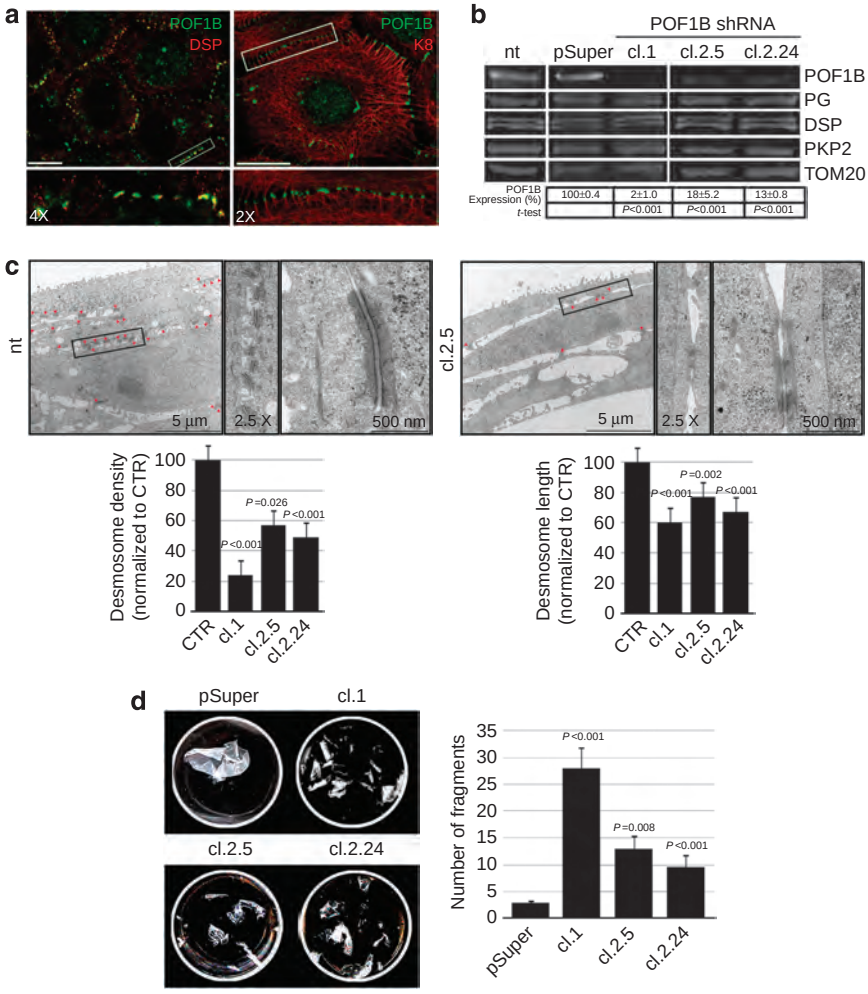

Figure 5. Defects of desmosomes in premature ovarian failure, 1B (POF1B)-knockdown HaCaT cells. (**a**) Confocal analysis of the indicated proteins in non-stratified HaCaT cells. (**b**) Western blot analysis of non-transfected (nt), pSuper, and POF1B-downregulated clones. Equal amounts of cell extracts were immunoprobed for the indicated markers, and TOM20 as control. (**c**) Transmission electron microscopy (TEM) and quantification of the indicated parameters. (**d**) Representative images and quantification of fragments obtained by the dispase assay. Data ± SEM ($n = 3$ independent experiments (**b**, **d**), (**c**) $n = 15$ sections each clone).

contact sites anchored to IFs (Figure 5a). Moreover, intracellular particles of POF1B distributed along K8 filaments were also clearly observed in subconfluent cells (not shown), further indicating a desmosomal localization of POF1B in these cells. The role of POF1B was then evaluated by the stable expression of POF1B shRNAs. Clones expressing shRNA2 (cl2.5 and 2.24) showed a great reduction in POF1B expression, and undetectable levels of the protein were found in the clone1 expressing the shRNA1 construct. No changes were found in cells stably transfected with the pSuper empty vector, and both expression and localization of desmosomal markers were maintained in POF1B-silenced clones (Figure 5b).

This result differed from that obtained in Caco-2 cells, where stable clones could not be generated and the transient downregulation of POF1B caused a marked effect on cell adhesion, leading to detachment of the silenced cells from the monolayer (Padovano *et al.*, 2011). The maintained morphology and expression of adhesion markers in silenced HaCaT cells could be explained by a function of POF1B in desmosomes dispensable for keratinocytes. To exclude this possibility we investigated whether the ultrastructure of desmosomes was maintained.

Defects in desmosome ultrastructure in HaCaT keratinocytes silenced for POF1B

Several defects in desmosomes were observed by conventional transmission electron microscopy in POF1B-silenced HaCaT keratinocytes. Quantitative analysis of the desmosome number and of the length of the plaque revealed a clear reduction of both parameters in all examined clones. Control (CTR) representing nontransfected and pSuper-expressing clones showed organized and well-defined junctions, whereas desmosomes of the silenced cells (cl.2.5) were discontinuous and with disorganized electron-dense plaques (Figure 5c), indicating that POF1B is indispensable for proper desmosome structure in HaCaT cells.

Adhesion defects in POF1B-silenced HaCaT keratinocytes

To assess the functional consequence on cell–cell adhesion of the ultrastructural defects found in desmosomes of POF1B-silenced keratinocytes, we measured the resistance to mechanical stress by the dispase fragmentation assay (Figure 5d). Treatment with the enzyme dispase allows cells to detach from the substrate, without affecting cell–cell adhesion, and the number of fragments obtained after mechanical stress provides a measure of the integrity of the epithelium (Huen *et al.*, 2002). Several fragments were measured in POF1B-silenced keratinocytes, and the number of fragments was inversely related to the level of expression of POF1B, thus indicating that POF1B expression is required to counteract mechanical stress. Fragmentation defects were not observed in pSuper-transfected clones (Figure 5d).

Localization of POF1B in desmosomes of normal and hyperproliferative epidermis

Given that results obtained in HaCaT cells may reflect differences between this proliferative cell line and normal epidermal keratinocytes *in situ*, we investigated the localization of POF1B in healthy skin and in hyperproliferative diseases of keratinocytes: basal cell carcinoma (BCC), squamous cell carcinoma (SCC), and psoriasis (PsO). The expression of POF1B is under the level of detection in basal and spinous layers (Figure 6a and Rizzolio *et al.*, 2007), and colocalization of POF1B with desmosome markers is restricted to upper layers in normal human epidermis (Figure 6b).

The restricted localization of POF1B does not rule against its desmosome association, as desmosome composition is different throughout the different layers of the epidermis (Simpson *et al.*, 2011), and desmosomal proteins with expressions confined in granular layers have been found and suggested to support terminal differentiation of the epidermis (Bazzi *et al.*, 2006).

Moreover, POF1B staining was not restricted to upper layers in hyperproliferative diseases of the epidermis, and, together with cytosolic staining, an average increase in POF1B staining at the cell periphery was consistently observed in all the analyzed samples. Surface localization was more homogenously found in BCCs than in PsOs, and a predominant cytosolic localization was found in four out of the six SCCs (three of which also displayed a cytosolic localization of desmosomal markers). Despite this variability in POF1B distribution in the different pathologies and within samples of the same pathology, perhaps related to the disease stage, POF1B significantly colocalized with DSP/DSG in these diseases (Figure 6b). Although the role of POF1B in desmosomes of normal and proliferative keratinocytes remains to be clarified, concerning POF1B expression, HaCaT cells exhibited higher similarity with these keratinocytes than with normal keratinocytes.

Collectively our data demonstrate an association of POF1B with the K8 component of IFs in Caco-2 cells, and localization and function of POF1B in desmosomes of Caco-2 and HaCaT cells. Moreover, although POF1B is normally excluded from desmosomes of the basal and spinous layers of the epidermis, we provide evidence for its desmosome localization in hyperproliferative keratinocytes of basal and suprabasal layers.

MATERIALS AND METHODS

Constructs

Generation and subcloning of human POF1B and shRNA1 or shRNA2 have been previously described (Padovano *et al.*, 2011). POF1B N-TER (aa 3–331 of POF1B) was generated by introducing an

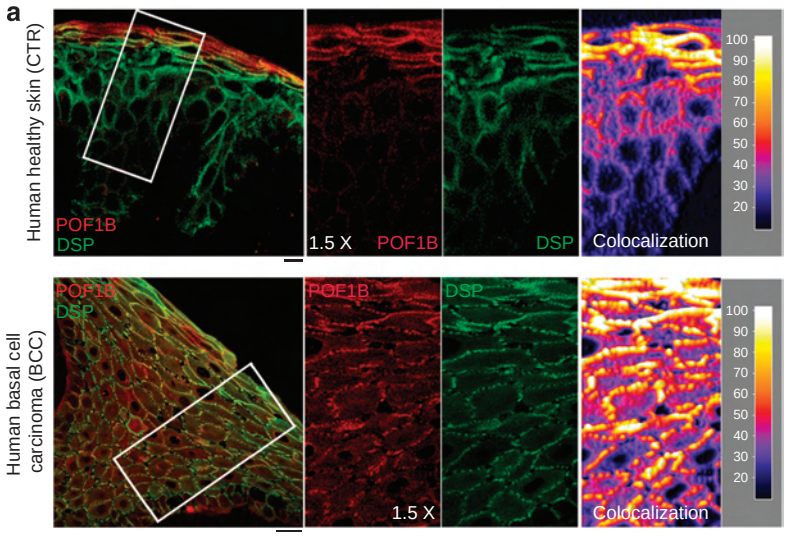

b

	MCC	±
CTR (upper)	0.682±0.075	+
CTR (lower)	0.180±0.064	–
BCC	0.828±0.039	+
SCC	0.718±0.049	+
PsO	0.714±0.042	+

Figure 6. Premature ovarian failure, 1B (POF1B) localization in normal and hyperproliferative human epidermis. (**a**) Confocal analysis of healthy and basal cell carcinoma (BCC) human samples stained for POF1B (red) and desmoplakin (DSP) (green). Individual channels are shown in the insets (×1.5 magnification). Interactive three-dimensional surface plot showing colocalization in false colors is shown on the right. Bars = 10 μm. (**b**) Manders' colocalization coefficient (MCC) of POF1B and DSP/desmoglein (DSG) signals in the upper layers and lower layers of control (CTR) healthy skin, BCC, squamous cell carcinoma (SCC), and psoriasis (PsO) was quantified as described in Materials and Methods. Colocalization is indicated for M2 values >0.5 (± column). Data are presented as mean ± SEM ($n = 4$, CTR and BCC; $n = 3$, PsO; $n = 2$, SCC).

in-frame stop codon at amino-acid position 331. A PCR was performed using GFP–POF1B as template and the following oligonucleotides: upper 5′-TCCGGACTGAATTCTCGATCGA-3′ and lower 5′-TAAGGATCCACTACACTAGTCGGA-3′; the product was inserted into the *Eco*RI–*Bam*HI restriction fragment of the mammalian expression vector pAcGFP1-C1. POF1B C-TER (aa 327–589 of POF1B) was obtained by carrying out a PCR with the following oligonucleotides: upper 5′-GTCTGAGAATTCACTCCGACTA-3′ and lower 5′-TCAGTTATCGAATTCCGGTG-3′; the PCR product was inserted into the mammalian expression vector pEGFP-C1 (*Eco*RI–*Bam*HI restriction fragment). mCherry-K8 was a kind gift from Dr R.E. Leube (Leube *et al.*, 2011). Double-stranded siRNA oligonucleotides against K8 were purchased from Sigma Aldrich (St Louis, MO). The sequence used was 5′-CAUGUUGCUUCGAGCCGUCTT-3′ (Long *et al.*, 2006).

Cell culture and transfections

Caco-2, IOSE523, and HaCaT cells were cultured in DMEM (Euroclone, Milan, Italy) supplemented with 1% L-glutamine (Sigma Aldrich), 1% penicillin–streptomycin (Sigma Aldrich), and 10% fetal bovine serum (Euroclone). All cell lines were maintained at 37 °C with 5% CO_2. Caco-2 and HaCaT cells were transfected using Polyethylenimine (PolyScience, Eppelheim, Germany) and IOSE523 cells using Lipofectamine 2000 (Invitrogen, Carlsbad, CA), according to the manufacturers' protocols. Stable cell lines were selected on the basis of growth in the antibiotic G418 (0.6 mg ml^{-1}) (Euroclone). In POF1B-silencing experiments, control cell lines were obtained by stable transfection with the pSuper empty vector (OligoEngine, Seattle, WA). In calcium deprivation conditions, Caco-2 cells were grown confluent in Petri dishes or glass coverslips for >6 days and switched to a low-calcium medium (free calcium DMEM + 10% dialyzed fetal bovine serum + 3 mM EGTA) for the indicated time.

Antibodies

Commercial primary antibodies used were mouse monoclonal anti-DSP (MAB-91920 SIC, Roma, Italy), anti-DSG1,2 (61002, PROGEN, Biotechnik, Heidelberg, Germany), anti-β-catenin (610153, BD Transduction Laboratories, Lexington, KY), anti-E-cadherin (610181), anti-PG (P8087), anti-K8 (C5301) and K14 (C8791) (Sigma Aldrich), anti-Claudin2 (32-5600, Zymed Laboratories, San Francisco, CA), and anti-PKP2 (651101, Santa Cruz Biotechnology, Santa Cruz, CA). The rabbit polyclonal antibodies used were as follows: anti-PAR3 (07–330, Upstate, Billerica, MA), anti-occludin (71–1500, Zymed Laboratories), and anti-TOM20 (sc-11415, Santa Cruz Biotechnology). Homemade rabbit polyclonal antibodies against mouse LIN7A, human POF1B, and β-catenin have been described elsewhere (Perego *et al.*, 2002; Rizzolio *et al.*, 2007; Massari *et al.*, 2009).

Immunoprecipitation and western blot analysis

Immunoprecipitation in Caco-2 cells using POF1B antibody was performed as previously described (Crespi *et al.*, 2012). Cell extracts and immunoprecipitates were solubilized in SDS denaturation buffer. Equal amounts of total protein, or 2% of the total extract (INPUT) and total immunoprecipitated proteins were separated by SDS-PAGE and transferred to nitrocellulose membranes. The blots were probed using the appropriate primary antibodies, followed by infrared-conjugated anti-rabbit IgG IRDye 800CW or anti-mouse IgG 680RD (LI-COR Bioscience, Lincoln, NE) as secondary reagents. Blots were scanned with the Odyssey CLx Infrared Imaging System (LI-COR, Bioscience), and the bands were quantified with Image Studio software (LI-COR).

Immunofluorescence

Cells grown on glass coverslips and human skin samples were processed for immunofluorescence as previously described (Rizzolio *et al.*, 2007; Padovano *et al.*, 2011). Patient consent for experiments was not required because the Italian Privacy Authority issued a general authorization for the use of retrospectively acquired human material on 1 March 2012. Images were acquired using a Zeiss LSM META (Carl Zeiss, Oberkochen, Germany) confocal microscope.

Conventional transmission electron microscopy

Cells were plated to confluence and cultured in a Petri dish for >8 days before processing and analysis as described elsewhere (Marino *et al.*, 2010).

The dispase mechanical fragmentation assay

Cells plated in triplicate were grown at high density for 7 days, and the assay was performed as described (Huen *et al.*, 2002). Briefly, cells were washed twice in phosphate-buffered saline, followed by treatment with 1 mg ml^{-1} dispase (STEMCELL technology, Milan, Italy). The dispase-detached sheet of cells was subjected to mechanical stress by 10–20 rapid inversions of the tube. The number of fragments was quantified using ImageJ software (NIH, Bethesda, MD).

Image and statistical analysis

Signal intensity quantification was evaluated using the ImageJ (NIH) ''surface plot'' and ''plot profile''. The percentage of staining-free membranes was obtained by signal quantification of 10-μm membranes randomly selected from ~10 cells. Quantification of POF1B colocalization with DSP/DSG in HaCaT and human skin samples was evaluated by Manders' colocalization coefficient *M2* as follows. Confocal acquisitions of five images of HaCaT cells or one image for each pathological sample (four samples for BCC and two and three samples each for SCC and PsO, respectively), selected on the basis of the surface localization of POF1B and DSP/DSG, were analyzed by selecting 5–10 regions of interest positively stained for desmosomal markers, each one corresponding to 10 μm of plasma membrane (~1 side of the cell). For healthy skin, three regions of interest from the upper layers and three from the lower layers have been selected from each image of the four samples. Regions of interest were analyzed with the ImageJ plugin JACoP. The Interactive three-dimensional Surface plots (ImageJ) were obtained from the colocalizing signal (MIN calculation between POF1B in red and DSP in green) of the selected images; the scale on the right indicates the intensity of fluorescence in arbitrary units. All quantitative data were expressed as mean ± SEM, and multiple comparisons among groups were carried out using Student's *t*-test in Prism software (GraphPad Prism Software, La Jolla, CA).

CONFLICT OF INTEREST

The authors state no conflict of interest.

ACKNOWLEDGMENTS

We thank Nelly Auersperg (British Columbia University, Vancouver, Canada) and Rudolph Leube (University of RWTH Aachen University, Aachen, Germany) for kindly providing IOSE523 cells and K8 cDNA, and the Monzino Foundation (Milan, Italy) for its generous gift of a Zeiss LSM META confocal

microscope. We thank Emily H. Stoops for her help in preparing the text. This work was partially supported by the PNR-CNR-aging program 2012–2014 and Unimi-FD-BIOMETRA-2014.

REFERENCES

Auersperg N, Maines-Bandiera SL, Dyck HG *et al.* (1994) Characterization of cultured human ovarian surface epithelial cells: phenotypic plasticity and premalignant changes. *Lab Invest* 71:510–8

Bazzi H, Getz A, Mahoney MG *et al.* (2006) Desmoglein 4 is expressed in highly differentiated keratinocytes and trichocytes in human epidermis and hair follicle. *Differentiation* 74:129–40

Bione S, Rizzolio F, Sala C *et al.* (2004) Mutation analysis of two candidate genes for premature ovarian failure, DACH2 and POF1B. *Hum Reprod* 19:2759–66

Bolling MC, Jonkman MF (2009) Skin and heart: une liaison dangereuse. *Exp Dermatol* 18:658–68

Brooke MA, Nitoiu D, Kelsell DP (2012) Cell-cell connectivity: desmosomes and disease. *J Pathol* 226:158–71

Capaldo CT, Farkas AE, Nusrat A (2014) Epithelial adhesive junctions. *F1000Prime Rep* 6:1

Crespi A, Ferrari I, Lonati P *et al.* (2012) LIN7 regulates the filopodium- and neurite-promoting activity of IRSp53. *J Cell Sci* 125:4543–54

Fey EG, Wan KM, Penman S (1984) Epithelial cytoskeletal framework and nuclear matrix-intermediate filament scaffold: three-dimensional organization and protein composition. *J Cell Biol* 98:1973–84

Garrod D, Kimura TE (2008) Hyper-adhesion: a new concept in cell-cell adhesion. *Biochem Soc Trans* 36:195–201

Green KJ, Getsios S, Troyanovsky S *et al.* (2010) Intercellular junction assembly, dynamics, and homeostasis. *Cold Spring Harb Perspect Biol* 2: a000125

Huen AC, Park JK, Godsel LM *et al.* (2002) Intermediate filament-membrane attachments function synergistically with actin-dependent contacts to regulate intercellular adhesive strength. *J Cell Biol* 159:1005–17

Kouklis PD, Hutton E, Fuchs E (1994) Making a connection: direct binding between keratin intermediate filaments and desmosomal proteins. *J Cell Biol* 127:1049–60

Kowalczyk AP, Green KJ (2013) Structure, function, and regulation of desmosomes. *Prog Mol Biol Transl Sci* 116:95–118

Lacombe A, Lee H, Zahed L *et al.* (2006) Disruption of POF1B binding to nonmuscle actin filaments is associated with premature ovarian failure. *Am J Hum Genet* 79:113–9

Leube RE, Moch M, Kolsch A *et al.* (2011) "Panta rhei": perpetual cycling of the keratin cytoskeleton. *Bioarchitecture* 1:39–44

Long HA, Boczonadi V, McInroy L *et al.* (2006) Periplakin-dependent re-organisation of keratin cytoskeleton and loss of collective migration in keratin-8-downregulated epithelial sheets. *J Cell Sci* 119:5147–59

Marino ML, Fais S, Djavaheri-Mergny M *et al.* (2010) Proton pump inhibition induces autophagy as a survival mechanism following oxidative stress in human melanoma cells. *Cell Death Dis* 1:e87

Massari S, Perego C, Padovano V *et al.* (2009) LIN7 mediates the recruitment of IRSp53 to tight junctions. *Traffic* 10:246–57

Nekrasova OE, Amargo EV, Smith WO *et al.* (2011) Desmosomal cadherins utilize distinct kinesins for assembly into desmosomes. *J Cell Biol* 195:1185–203

Oriolo AS, Wald FA, Ramsauer VP *et al.* (2007) Intermediate filaments: a role in epithelial polarity. *Exp Cell Res* 313:2255–64

Padovano V, Lucibello I, Alari V *et al.* (2011) The POF1B candidate gene for premature ovarian failure regulates epithelial polarity. *J Cell Sci* 124: 3356–68

Perego C, Vanoni C, Massari S *et al.* (2002) Invasive behaviour of glioblastoma cell lines is associated with altered organisation of the cadherin-catenin adhesion system. *J Cell Sci* 115:3331–40

Protonotarios N, Tsatsopoulou A, Patsourakos P *et al.* (1986) Cardiac abnormalities in familial palmoplantar keratosis. *Br Heart J* 56:321–6

Rampazzo A (2006) Genetic bases of arrhythmogenic right ventricular cardiomyopathy. *Heart Int* 2:17–26

Riva P, Magnani I, Fuhrmann Conti AM *et al.* (1996) FISH characterization of the Xq21 breakpoint in a translocation carrier with premature ovarian failure. *Clin Genet* 50:267–9

Rizzolio F, Bione S, Villa A *et al.* (2007) Spatial and temporal expression of POF1B, a gene expressed in epithelia. *Gene Expr Patterns* 7: 529–34

Simpson CL, Patel DM, Green KJ (2011) Deconstructing the skin: cytoarchitectural determinants of epidermal morphogenesis. *Nat Rev Mol Cell Biol* 12:565–80

Stappenbeck TS, Green KJ (1992) The desmoplakin carboxyl terminus coaligns with and specifically disrupts intermediate filament networks when expressed in cultured cells. *J Cell Biol* 116:1197–209

Wallis S, Lloyd S, Wise I *et al.* (2000) The alpha isoform of protein kinase C is involved in signaling the response of desmosomes to wounding in cultured epithelial cells. *Mol Biol Cell* 11:1077–92

Yin T, Green KJ (2004) Regulation of desmosome assembly and adhesion. *Semin Cell Dev Biol* 15:665–77